Progress In Electromagnetics Research M, Vol. 65, 19–27, 2018

An Annular-Ring Miniaturized Stopband Frequency Selective Surface with Ultra-Large Angle of Incidence

Kunzhe Zhang*, Wen Jiang, Junyi Ren, and Shuxi Gong

Abstract—An annular-ring element for building a miniaturized bandstop frequency selective surface (FSS) structure which possesses a superior performance with respect to electromagnetic wave polarizations and incident angles is introduced in this paper. The proposed element has prominent miniaturization characteristics with a unit dimension of $0.061\lambda \times 0.061\lambda$, where λ represents the free-space wavelength corresponding to resonant frequency. Miniaturization of the proposed FSS element is achieved by constructing special meandered strips in geometry and arranging lumped components between the elements. The advantage of this method lies in its great simplicity in tuning the resonant frequency of FSS by adjusting values of the printed capacitors rather than rebuilding the geometry. The obtained FSS also exhibits a stable performance in terms of angle stability and polarization insensitivity. Prototypes of the proposed FSS are fabricated and measured to verify design method. Measurements are well in line with simulation results.

1. INTRODUCTION

Frequency selective surface (FSS) generally refers to a two-dimensional or three-dimensional periodic structure consisting of periodically arranged metal sheets or slots etched on metal screens [1]. It is widely used in fields such as satellite communication [2], antenna beam-steering [3], electromagnetic shielding [4], meta-materials integration [5] and radar cross section (RCS) reduction [6–8] based on its spatial filter characteristics of electromagnetic (EM) waves such as bandpass or bandstop response. However, performance requirements for FSSs are different according to application environments. For example, miniaturization is necessary when FSSs are arranged in a limited space. Angular stability is an essential factor when designing a conformal FSS. Other characteristics such as polarizations insensitivity and high selectivity are also needed. To meet such requirements, different structures are adopted, and many good results are obtained [9–11].

Stopband FSSs are more widely used among these applications. They can reflect incident EM waves in specified frequencies and transmit EM waves in other frequency bands. A lot of structures have been introduced in the previous literature. A three-dimensional structure implemented by using via holes in a multilayer printed circuit board structure was proposed in [12] to construct a miniaturized unit cell with the characteristic of incident angular stability. The proposed FSS can maintain a stable performance with incident angle up to 60° for both TE and TM polarizations. Another miniaturized 3D bandstop FSS introduced in [13] had a thin thickness geometry, and angular stability could be up to 30°. In [14], a 2.5-dimensional structure was proposed and analyzed, where successive segments of the loop were placed alternately on two surfaces of a substrate and then interconnected through vias. The angular stability of this structure was 60° for TE and TM polarizations. In [15], an FSS with miniaturized resonator element was proposed. Its miniaturization was achieved by coupling two meandered wire

Received 10 January 2018, Accepted 14 February 2018, Scheduled 24 February 2018
* Corresponding author: Kunzhe Zhang (zhangkunzhe@hotmail.com).
The authors are with the National Key Laboratory of Antennas and Microwave Technology, Xidian University, Xi'an, Shaanxi 710071, China.

resonators separated by single thin substrate. The angular response stability of this FSS could be up to 80° for TE and TM polarizations. Although the above-mentioned structures could exhibit an excellent performance with respect to incident angles, they had the same drawbacks of complicated geometry and difficult fabrication. A single-layer FSS designed utilizing fractal method was described in [16]. It exhibited great stability with the incident angle ranging from 0° to 80° for both TE and TM polarizations. However, optimization of this model was a trouble when tuning the resonant frequency, which means that the idea was not a good choice in practice.

In this paper, we propose a stopband miniaturized FSS with simple geometry and superior performance. The proposed FSS is a single-layer structure. Miniaturization of the designed FSS was implemented by constructing special meandered strips in geometry and arranging lumped capacitors between unit cells. The difference between this method and previous method is that the tuning of resonant frequency can be realized by adjusting values of lumped capacitors instead of changing the physical dimension of structure. Moreover, the magnitude variety of capacitance has little effect on the performance of angular stability. Therefore, this method is useful in designing FSSs with different operating frequencies, which is of great significance in practical applications. Additionally, the proposed FSS is symmetrical in nature, thereby providing identical response for both TE and TM polarizations.

2. FSS DESIGN

2.1. Structure Design and Performance

Figure 1 illustrates the array structure and unit cell geometry, respectively, of the proposed FSS (FSS1). The top metal patches are made of copper and printed on the top surface of a thin F_4BM substrate with a relative permittivity 2.65, loss tangent 0.002, and thickness 1 mm. The unit cell is composed of a circular loop in the center and four identical meandered wires arranged in diagonals, which are connected through metallic strips. Meandered wires are widely used in designing miniaturized FSS as reported in previous literature. In our design, they are also designed carefully to achieve the same purpose. The proposed unit cell is then arranged in periodic pattern, which are connected with the other through diagonal pairs. The purpose of arranging unit cells in diagonal is that a compact arrangement can be obtained in this way, which is beneficial for miniaturization. In addition, since the geometry of a unit cell is center rotation symmetry, the whole structure could show a low sensitivity to the polarization of incident waves. Other geometrical dimensions of unit cell are as follows: $P = 22\,\text{mm}$, $g = 0.4\,\text{mm}$, $d = 4\,\text{mm}$, $r = 3.2\,\text{mm}$, $K = 15.5\,\text{mm}$, $w = 0.6\,\text{mm}$, $w1 = 0.5\,\text{mm}$, $w2 = 0.3\,\text{mm}$, $\alpha = 45\,\text{deg}$, $\beta = 60\,\text{deg}$, $\gamma = 180\,\text{deg}$.

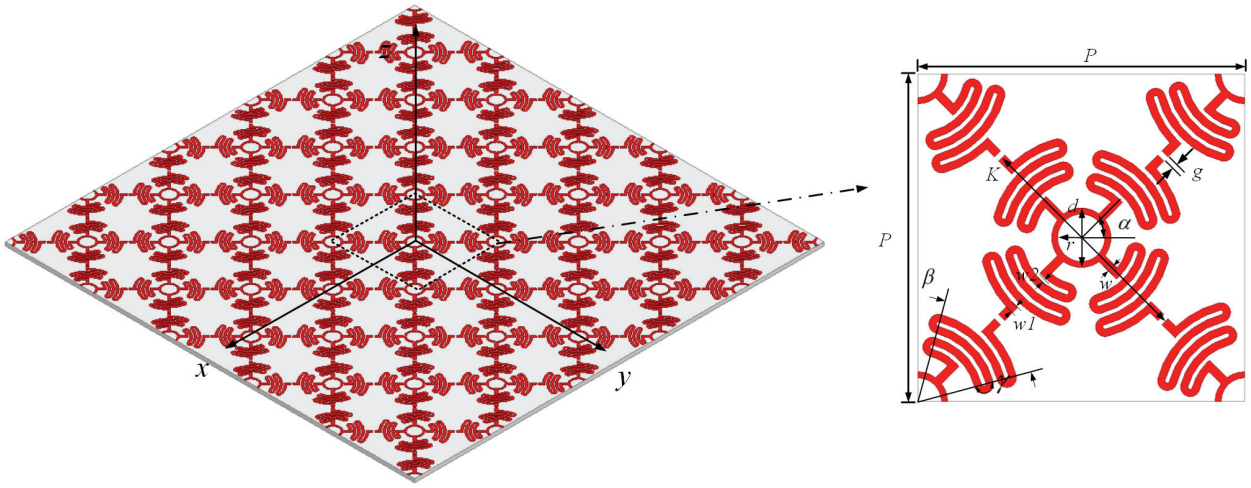

Figure 1. Perspective view of the FSS and enlarged view of unit cell.

The performance of FSS1 has been simulated in High Frequency Solution Solver (*HFSS*), and simulation results under transverse electronic (TE) and transverse magnetic (TM) polarizations with different incident angles are plotted in Fig. 2. It can be observed that this structure resonates at 3.65 GHz at normal incidence. Meanwhile, it offers almost total reflection at resonant frequency, and the −10 dB bandwidth is 0.45 GHz. The ratio of unit cell size to λ is 0.189, where λ is the free space wavelength corresponding to the resonant frequency. The largest deviation of resonant frequency is 0.05 GHz for TE polarization and 0.03 GHz for TM polarization, respectively, when the incident angle ranges from 0° to 85°, which indicates that the designed FSS1 has a fairly stable performance.

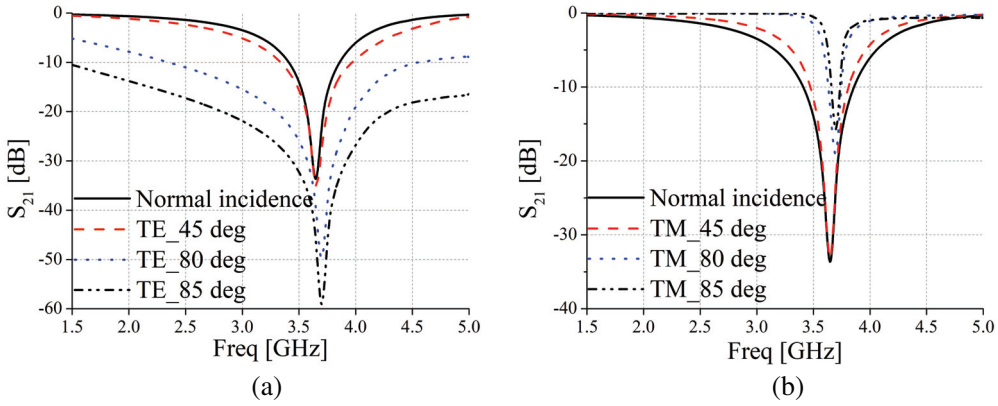

Figure 2. Simulated S_{21} of FSS1 under (a) TE polarization and (b) TM polarization.

2.2. Miniaturization Realization

Although the FSS1 described in Section 2.1 exhibits a stable performance with respect to incident angles for both TE and TM polarizations, its miniaturization feature is not prominent. Except for the special geometry of a unit cell, we utilize lumped capacitors (Ct) between unit cells in design to pursue a further miniaturization, as shown in Fig. 3. These lumped capacitors are printed in the slots present within the diagonals. The Lumped RLC Boundary in *HFSS* is used to simulate the arranged lumped capacitors and obtained results when $Ct = 0.25$ pF (FSS2) is plotted in Fig. 4.

It can be seen from Fig. 4 that the proposed FSS2 shows a bandstop response at the frequency of 1.46 GHz at normal incidence, and the −10 dB bandwidth is 0.57 GHz. In this case, the ratio of unit cell size to λ is 0.075, which is reduced by about 60% compared to that of FSS1. In addition, the performance of angular stability has been slightly improved. The largest frequency deviation is 0.01 GHz for both TE and TM polarizations when the incident angle ranges from 0° to 85°.

An equivalent circuit model (ECM) is developed to explain the method of loading lumped capacitors, as shown in Fig. 3. According to Munk's theory, FSS1 topology can be modelled by a series LC circuit model. It shows a bandstop response, and the resonant frequency can be approximately computed according to Equation (1), where the equivalent inductance and capacitance of this circuit model depend on physical parameters of the given geometry structure. However, the resonant frequency

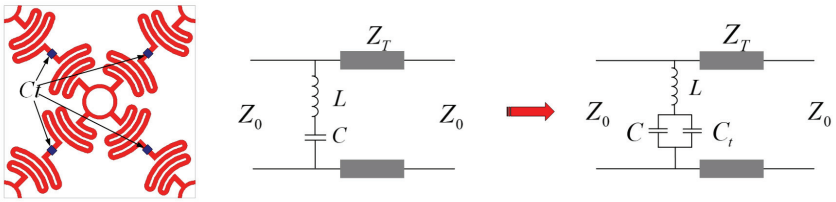

Figure 3. Top view of FSS unit cell (FSS2) and the evolution of ECMs.

will be calculated according to Equation (2) when lumped capacitors Ct are mounted. Obviously, in the case of the same geometry structure, the resonant frequency of FSS2 is smaller than that of FSS1, thereby achieving the purpose of miniaturization.

$$f = 1/2\pi\sqrt{LC} \tag{1}$$

$$f = 1/2\pi\sqrt{L(C+C_t)} \tag{2}$$

To validate the equivalent circuit model of FSS, simulated results obtained from the circuit model and full wave simulation are compared in Fig. 5. The initial inductance in the circuit model can be calculated using Equation (3) as described in [14]:

$$L = \mu_0\mu_{eff}\frac{D}{2\pi}\ln\left(\frac{1}{\sin\left(\pi w/2D\right)}\right) \tag{3}$$

where D is the length of the meandered strips, w the width of meandered strips, μ_0 the free space permeability, and μ_{eff} the effective permeability.

Values of the capacitance in the circuit can be obtained from Equation (1), where f represents the resonant frequency. The circuit model is then simulated and optimized in Advanced Design System (ADS). The final optimized values are determined as: $Z_0 = 377\,\Omega$, $Z_t = Z_0/\sqrt{\varepsilon_r}$, $L = 19.80\,\text{nH}$ and $C = 0.09\,\text{pF}$. It can be observed from Fig. 5 that the results from ADS agree well with that from $HFSS$. In fact, this is a key feature of our method, which efficiently enables the design of a miniaturized FSS with stable performance by introducing different capacitances.

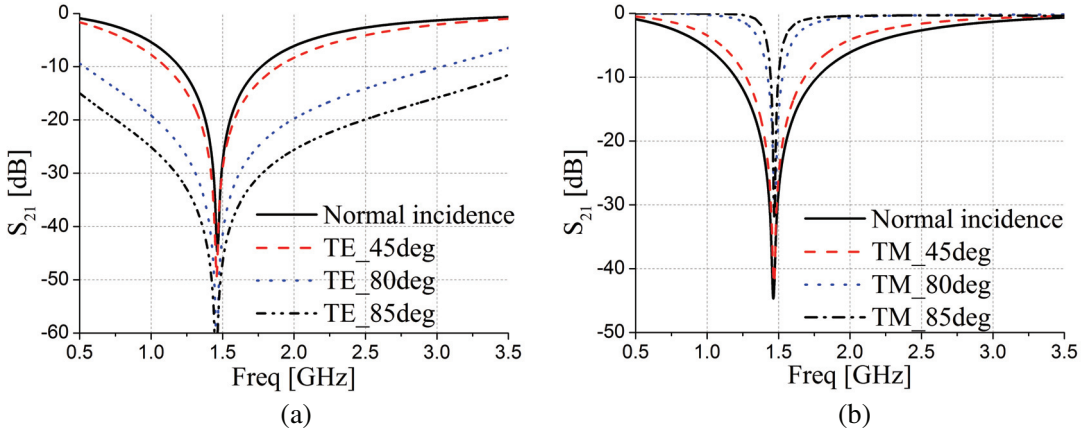

Figure 4. Simulated S_{21} of FSS2 under (a) TE polarization and (b) TM polarization when $Ct = 0.25\,\text{pF}$.

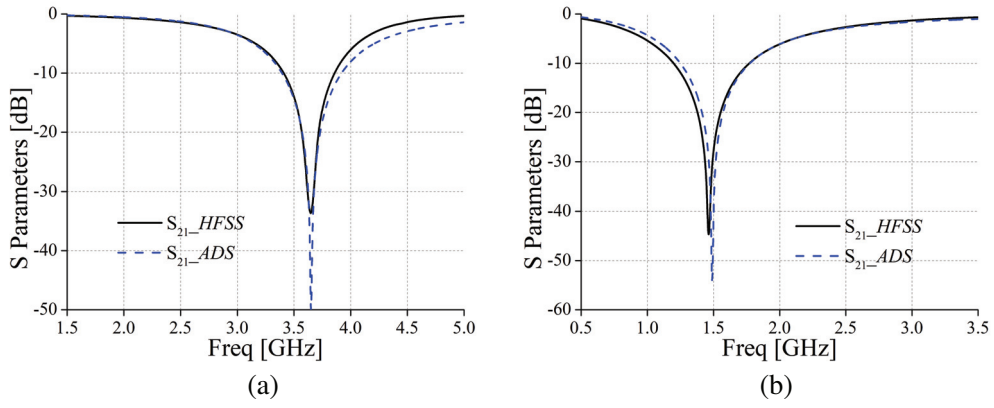

Figure 5. Comparison of results from $HFSS$ and from ADS of (a) FSS1 and (b) FSS2.

3. RESONANT FREQUENCY TUNING

Another advantage of this method lies in its flexibility in designing miniaturized bandstop FSS resonating at other frequencies by adopting lumped capacitors with different capacitance values instead of changing the structure. As we know, most of the miniaturized FSSs have special requirements for their geometry structures. The resonant frequency would be determined once the structures are established, which means that making changes based on the present structure to design another FSS resonating at other frequencies will be very difficult, and it will also be quite tedious to do a completely new design. From the description of the mentioned ECM, it can be learned that the resonant frequency of the proposed FSS can be adjusted by employing different Ct values instead of rebuilding geometry, which means that frequency tuning can be achieved simply in our design. In addition, since no geometry has been changed during this process, the characteristic of angular stability and polarizations insensitivity to EM waves can be maintained well. Furthermore, if varactor diodes with bias network are used instead of these capacitors, an active frequency selective surface (AFSS) with tunable frequency can be obtained.

As a comparison, another FSS (FSS3) with the same geometry but a different Ct ($Ct = 1.0\,\text{pF}$) is simulated in *HFSS*, and results are plotted in Fig. 6. As can be seen, the resonant frequency of FSS3 is 1.18 GHz at normal incidence, and the $-10\,\text{dB}$ bandwidth is 0.59 GHz. The ratio of unit cell size to λ is 0.061, which is reduced by about 68% and 19%, respectively, compared with FSS1 and FSS2. The largest deviation of resonant frequency is about 0.05 GHz for TE polarization and 0.07 GHz for TM polarization, respectively, when the incident angle ranges from 0° to 85°. Compared with the previous two FSSs, the characteristic of angular stability gets worse slightly. The main reason for this deterioration may be considered from the values of equivalent inductance and capacitance. As we know, the equivalent inductance and capacitance will change with increasing the incident angles while the lumped capacitance Ct does not. Therefore, the shift of resonant frequency at different incident angles as well as polarizations varies with the values of lumped capacitance Ct. It is difficult to predict this deterioration through numerical analysis. Despite the deficiencies, the design method can be verified well by these three FSSs. Performances of these three FSSs are also listed in Table 1 to provide a more intuitive comparison.

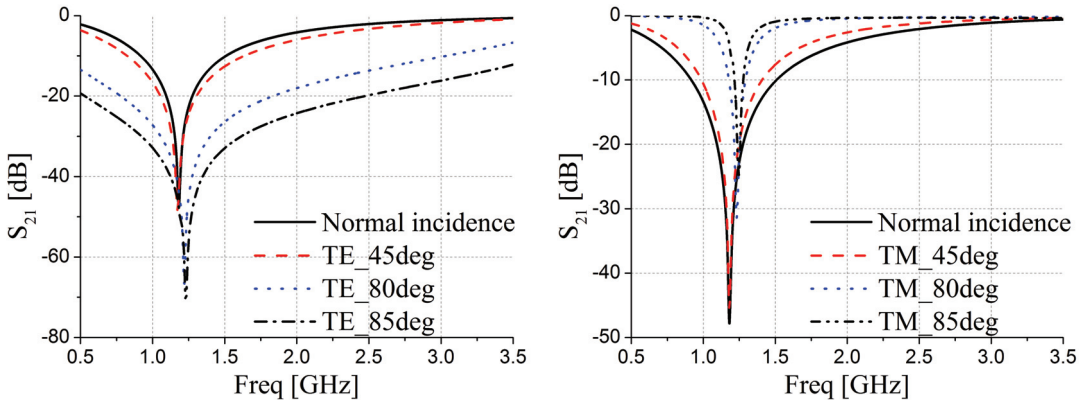

Figure 6. Simulated S_{21} of FSS3 under (a) TE polarization and (b) TM polarization when $Ct = 1.0\,\text{pF}$.

The proposed FSS can be used as a sub-reflector in a Cassegrain antenna system because of its stable performance in terms of polarization and incident angle of EM waves. The useful EM waves from the feed can be reflected by the sub-reflector to the main reflector while other EM waves will not be reflected. In addition, since the resonant frequency of FSS can be tuned easily using this method, it will be very convenient when the antenna needs to convert the operating frequency. Moreover, the method is useful for the design of FSS elements operating at frequency of 3G, 4G and 5G commercial bands.

Table 1. Comparison of the three proposed FSSs.

Sample	Resonant Frequency (GHz)	Unit Cell Size	Bandwidth (GHz)	Frequency Deviation (GHz)
FSS1	3.65	0.189λ	0.45	TE:0.05
				TM:0.03
FSS2	1.46	0.075λ	0.57	TE:0.01
				TM:0.01
FSS3	1.18	0.061λ	0.59	TE:0.05
				TM:0.07

*λ represents the free-space wavelength corresponding to resonant frequency.

4. EXPERIMENT AND DISCUSSION

In order to validate the design methodology, prototypes of the proposed miniaturized FSS architectures are manufactured using printed circuit board (PCB) technology, as shown in Fig. 7. The overall size of the prototype is 308 mm $*$ 308 mm, on which 378 unit cells and 1512 lumped capacitors are printed. The lumped capacitors mounted in the FSS are *LQP* series capacitors with 0402-package from Murata Company. Experiment is carried out in a microwave anechoic chamber under the guidance of free-space measurement system. We calibrate the measurement system first and then test transmission coefficients of the fabricated FSSs. Fig. 8, Fig. 9 and Fig. 10 show both the measured and simulated results under normal incidence and oblique 80° as well as both TE and TM polarizations for FSS1, FSS2 and FSS3, respectively. It can be observed that measured curves of these prototypes have a good agreement

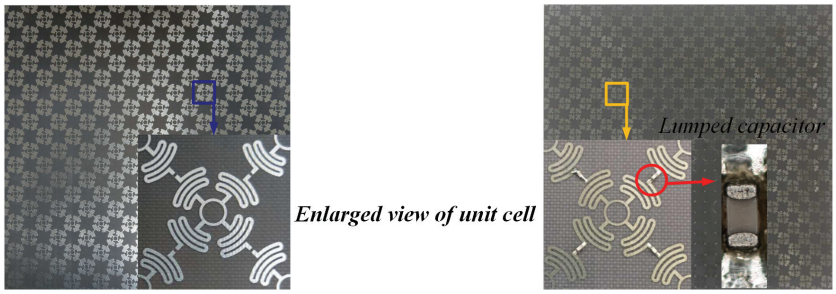

Figure 7. Pictures of fabricated FSS structures.

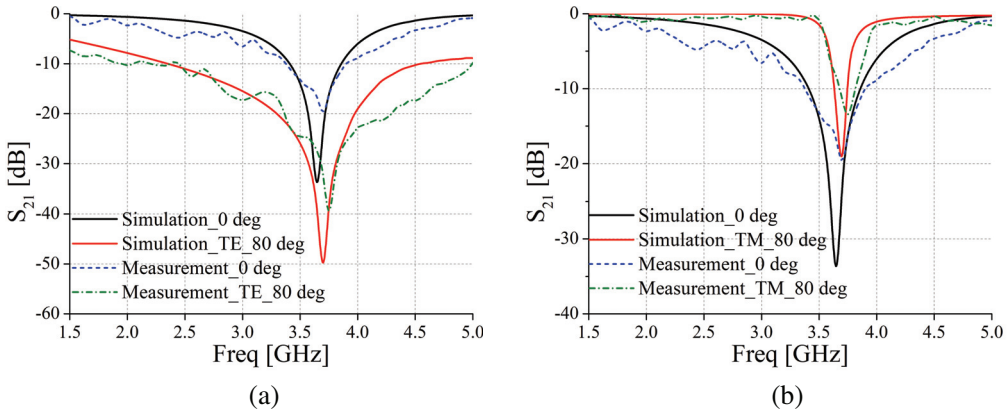

Figure 8. Simulated and measured results of FSS1 for (a) TE polarization and (b) TM polarization.

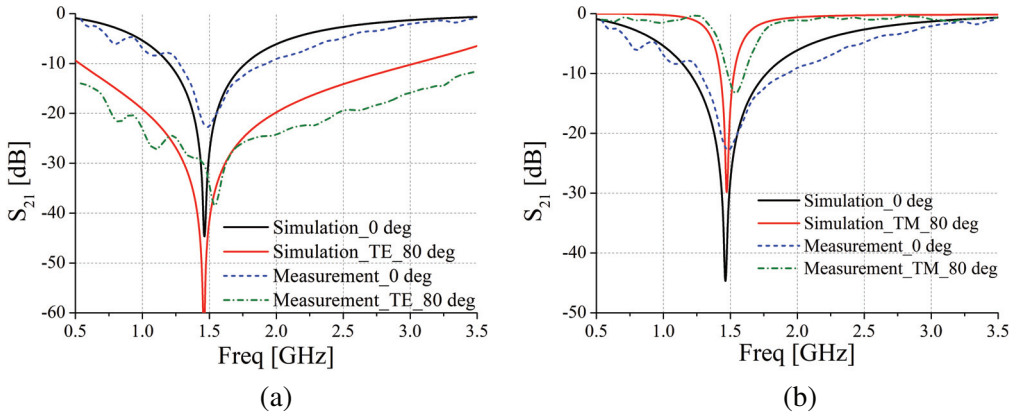

Figure 9. Simulated and measured results of FSS2 for (a) TE polarization and (b) TM polarization.

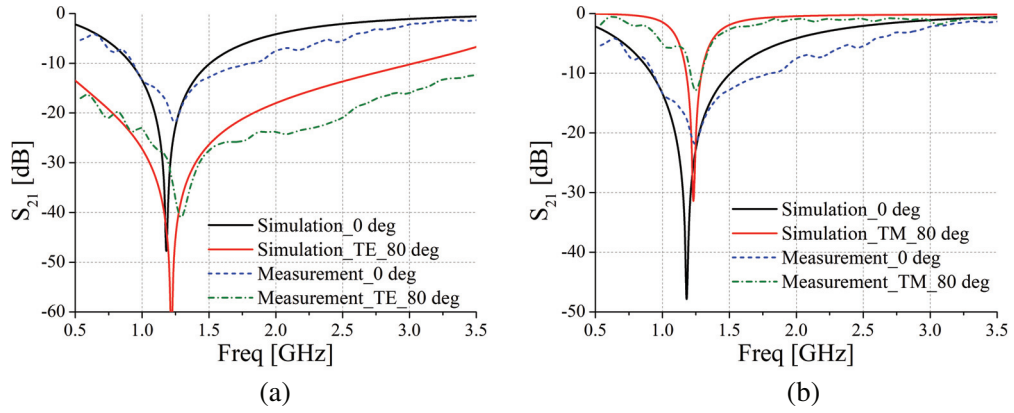

Figure 10. Simulated and measured results of FSS3 for (a) TE polarization and (b) TM polarization.

Table 2. Performance comparison of the designed FSS with the state-of-the-art.

Referenced	Unit cell size	Resonant Frequency	Unit cell Characteristic	Angular stability	Frequency deviation
[12]	0.205λ	6.5 GHz	3-layer structure	60°	0.09 GHz
[14]	0.062λ	1.89 GHz	2-layer structure + lot of metal vias	60°	0.06 GHz
[15]	0.067λ	3.33 GHz	2-layer structure	80°	0.06 GHz
[16]	0.116λ	7GHz	Single layer	80°	0.08 GHz
This work	0.061λ	1.18 GHz	Single layer + components	85°	0.07 GHz

*λ represents the free-space wavelength corresponding to resonant frequency.

with the simulated results despite that the measured results have slight frequency deviations. These slight frequency deviations are mainly caused by factors such as fabrication errors, measurement system errors and the deviations of marked capacitance of components. However, existence of slight deviations is acceptable and does not affect the validation of the proposed method.

Performance of the proposed FSS is also compared with the state-of-the-art in Table 2. It can be seen that our work has the best performance in terms of miniaturization, angular stability. Although the FSSs in [15, 16] have neatly same angular stability as our design, there is no doubt that our design has the simplest geometry. In addition, our proposed model can be easily reconstructed when tuning the resonant frequency, something that other mentioned models cannot do.

5. CONCLUSION

An annular-ring miniaturized frequency selective surface with stable performance of angular stability and polarization insensitivity to EM waves is proposed in this paper. The designed FSS can maintain a good resonant characteristic in both TE and TM polarizations when the incident angles are up to 85°. Prototypes of the designed FSS are fabricated and measured to verify this method. Measurements show a good agreement with simulation results. Besides its miniaturization, the resonant frequency can be easily adjusted using this method without changing the geometry. Moreover, the obtained FSSs also have a stable performance with respect to incident angles and EM wave polarizations, which means that this method has wide application in practice.

ACKNOWLEDGMENT

This work was supported by the National Basic Research Program of China-973 program 2015CB857100, National Natural Science Foundation of China (No. 61401327, 61471278, 61601350), Foundation of Chinese Academy of Space Technology (CAST 2015-11), and Natural Science Basic Research Plan in Shaanxi Province of China (No. 2015JQ6217).

REFERENCES

1. Munk, B. A., *Frequency Selective Surfaces: Theory and Design*, Wiley, New York, NY, USA, 2000.
2. Chaharmir, M. R. and J. Shaker, "Design of a multilayer X-/Ka-band frequency-selective surface-backed reflectarray for satellite applications," *IEEE Trans. Antennas Propag.*, Vol. 63, 1255–1262, 2015.
3. Boccia, L., I. Russo, G. Amendola, and G. Di Massa, "Tunable frequency-selective surfaces for beam-steering applications," *Electronics Letters*, Vol. 45, 1213–1215, 2009.
4. Sivasamy, R., M. Kanagasabai, et al., "A novel shield for GSM 1800 MHz band using frequency selective surface," *Progress In Electromagnetics Research Letters*, Vol. 38, 193–199, 2013.
5. Ghosh, S. and K. V. Srivastava, "An equivalent circuit model of FSS-based metamaterial absorber using coupled line theory," *IEEE Antennas Wireless. Propag. Lett.*, Vol. 14, 511–514, 2015.
6. Zheng, J. and S. J. Fang, "A new method for designing low RCS patch antenna using frequency selective surface," *Progress In Electromagnetics Research Letters*, Vol. 58, 125–131, 2016.
7. Joozdani, M. Z., M. K. Amirhosseini, and A. Abdolali, "Wideband radar cross-section reduction of patch array antenna with miniaturized hexagonal loop frequency selective surface," *Electronics Letters*, Vol. 52, 767–768, 2016.
8. Xie, D., X. Liu, H. Guo, et al., "Wideband absorber with multi-resonant gridded-square FSS for antenna RCS reduction," *IEEE Antennas Wireless. Propag. Lett.*, Vol. 16, 629–632, 2017.
9. Edalati, A. and K. Sarabandi, "Reflectarray antenna based on grounded loop-wire miniaturized element frequency selective surfaces," *Microwaves Antennas & Propagation IET*, Vol. 8, 973–979, 2014.
10. Liu, X., Q. Wang, W. Zhang, et al., "On the improvement of angular stability of the 2nd-order miniaturized FSS structure," *IEEE Antennas Wireless. Propag. Lett.*, Vol. 15, 826–829, 2016.
11. Rahmati, B. and H. R. Hassani, "Multiband metallic frequency selective surface with wide range of band ratio," *IEEE Trans. Antennas Propag.*, Vol. 63, 3747–3753, 2015.
12. Lee, I. G. and I. P. Hong, "3D frequency selective surface for stable angle of incidence," *Electronics Letters*, Vol. 50, 423–424, 2014.
13. Li, B. and Z. X. Shen, "Miniaturized bandstop frequency-selective structure using stepped impedance resonators," *IEEE Antennas Wireless. Propag. Lett.*, Vol. 12, 1112–1115, 2012.
14. Hussain, T., Q. Cao, J. Kayani, et al., "Miniaturization of frequency selective surfaces using 2.5-dimensional knitted structures: Design and synthesis," *IEEE Trans. Antennas Propag.*, Vol. 65, 2405–2412, 2017.

15. Azemi, G. W., "Angularly stable frequency selective surface with miniaturized unit cell," *IEEE Microwave & Wireless Components Lett.*, Vol. 25, 454–456, 2015.
16. Zhao, Z., H. Shi, J. Guo, et al., "A stop-band frequency selective surface with ultra-large angle of incidence," *IEEE Antennas Wireless. Propag. Lett.*, Vol. 16, 553–556, 2017.